

# Self-Similar Accretion Flows with Convection

Ramesh Narayan

Harvard-Smithsonian Center for Astrophysics, 60 Garden Street, Cambridge MA 02138, U. S. A.

Igor V. Igumenshchev<sup>1</sup>, Marek A. Abramowicz<sup>2</sup>

Institute for Theoretical Physics, Goteborg University and Chalmers University of Technology, 412 96  
Goteborg, Sweden

## ABSTRACT

We consider height-integrated equations of an advection-dominated accretion flow (ADAF), assuming that there is no mass outflow. We include convection through a mixing length formalism. We seek self-similar solutions in which the rotational velocity and sound speed scale as  $R^{-1/2}$ , where  $R$  is the radius, and consider two limiting prescriptions for the transport of angular momentum by convection. In one limit, the transport occurs down the angular velocity gradient, so convection moves angular momentum outward. In the other, the transport is down the specific angular momentum gradient, so convection moves angular momentum inward. We also consider general prescriptions which lie in between the two limits.

When convection moves angular momentum outward, we recover the usual self-similar solution for ADAFs in which the mass density scales as  $\rho \propto R^{-3/2}$ . When convection moves angular momentum inward, the result depends on the viscosity coefficient  $\alpha$ . If  $\alpha > \alpha_{crit1} \sim 0.05$ , we once again find the standard ADAF solution. For  $\alpha < \alpha_{crit1}$ , however, we find a non-accreting solution in which  $\rho \propto R^{-1/2}$ . We refer to this as a “convective envelope” solution or a “convection-dominated accretion flow.”

Two-dimensional numerical simulations of ADAFs with values of  $\alpha \lesssim 0.03$  have been reported by several authors. The simulated ADAFs exhibit convection. By virtue of their axisymmetry, convection in these simulations moves angular momentum inward, as we confirm by computing the Reynolds stress. The simulations give  $\rho \propto R^{-1/2}$ , in good agreement with the convective envelope solution. The  $R^{-1/2}$  density profile is not a consequence of mass outflow. The relevance of these axisymmetric low- $\alpha$  simulations to real accretion flows is uncertain.

*Subject headings:* Accretion, accretion disks — convection — hydrodynamics — turbulence

## 1. Introduction

Advection-dominated accretion flows (ADAFs, see Narayan, Mahadevan & Quataert 1998 and Kato, Fukue & Mineshige 1998 for reviews) were introduced to astrophysics by Ichimaru (1977) and have been studied extensively in the last few years (Narayan & Yi 1994, hereafter NY, Abramowicz et al. 1995, Narayan & Yi 1995a, 1995b, Chen et al. 1995). The recent interest in ADAFs has been stimulated to a large extent by the fact that these flows provide a natural explanation for many phenomena associated with low-luminosity accreting black holes (Narayan et al. 1998). ADAFs are also relevant for understanding black holes with super-Eddington accretion (Abramowicz et al. 1988).

---

<sup>1</sup>On leave from Institute of Astronomy, 48 Pyatnitskaya St., 109017 Moscow, Russia

<sup>2</sup>also: Laboratorio Interdisciplinare SISSA and ICTP, Trieste, Italy

NY derived an analytic self-similar solution for an ADAF which has provided considerable insight into the properties of these flows. A number of authors have extended this work and obtained related solutions (e.g. Narayan & Yi 1995a, Honma 1996, Kato & Nakamura 1998, Blandford & Begelman 1999, Manmoto et al. 2000).

NY showed that the entropy of the accreting gas in an ADAF increases towards smaller radii. They argued that an ADAF is therefore likely to be convectively unstable. The convective instability was confirmed by Igumenshchev, Chen & Abramowicz (1996) using numerical simulations. More detailed simulations have been reported by Igumenshchev & Abramowicz (1999) and Stone, Pringle & Begelman (1999).

Although NY recognized the importance of convection, they incorporated its effects only schematically in the derivation of their self-similar solution. We present a more detailed discussion here. We show that, depending on whether convective turbulence moves angular momentum outward or inward, the nature of ADAFs may be very different. We use this insight to interpret the numerical simulations of Igumenshchev and others. A related analysis is presented in the accompanying paper by Quataert & Gruzinov (2000, hereafter QG).

## 2. Self-Similar Scalings

Our analysis and notation closely follow the discussion given in NY. We work with height-integrated equations (see Narayan & Yi 1995a for an interpretation of height-integration). We assume that there is no significant mass outflow from the ADAF, i.e. that the mass accretion rate  $\dot{M}$  is independent of radius  $R$ . The Keplerian angular velocity is  $\Omega_K = (GM/R^3)^{1/2}$  and the corresponding linear velocity is  $v_K = R\Omega_K = (GM/R)^{1/2}$ , where  $M$  is the mass of the accreting star (black hole) and  $R$  is the cylindrical radius.

We seek a self-similar solution which satisfies the following scalings for the angular velocity  $\Omega$ , the isothermal sound speed  $c_s$  and the scale height  $H$ :

$$\begin{aligned}\Omega(R) &= \Omega_0 \Omega_K \propto R^{-3/2}, \\ c_s^2(R) &= c_0^2 v_K^2 \propto R^{-1}, \\ H(R) &= c_s / \Omega_K = c_0 R,\end{aligned}$$

where  $\Omega_0$  and  $c_0$  are dimensionless constants to be determined. We write the density  $\rho$  as

$$\rho(r) = \rho_0 R^{-a},$$

so that the pressure scales as

$$p(R) = \rho c_s^2 \propto R^{-1-a}.$$

The index  $a$  is equal to  $3/2$  in the original self-similar solution of NY; we reproduce this scaling in §4. However, as we show in §§5.2, 6, under appropriate conditions a very different solution is possible, which has  $a = 1/2$ .

As in NY, we apply the conservation laws of mass, radial momentum, angular momentum and energy to solve for the various unknowns. Mass conservation requires that  $\rho v R H$  be independent of  $R$ , where  $v$  is the radial velocity. This gives the following scaling for  $v$ :

$$v(R) \propto R^{a-2} \propto R^{a-3/2} v_K.$$

In the radial momentum equation, we assume for simplicity that  $v^2 \ll v_K^2$ , which corresponds to the condition that the Shakura-Sunyaev viscosity coefficient  $\alpha$  is small:  $\alpha^2 \ll 1$ . This allows us to ignore the ram pressure term  $vdv/dR$ . We also ignore the gradient of the turbulent pressure. The radial momentum equation then simplifies to a simple balance between gravity, centrifugal force and thermal pressure gradient. This gives

$$\Omega_K^2 R - \Omega^2 R = -\frac{1}{\rho} \frac{dp}{dR} = (a+1)c_0^2 \frac{v_K^2}{R},$$

which leads to the condition

$$\Omega_0^2 = 1 - (a+1)c_0^2. \quad (1)$$

Since we require  $\Omega_0^2 \geq 0$ , we see that  $c_0^2 \leq 2/5$  for  $a = 3/2$  and  $c_0^2 \leq 2/3$  for  $a = 1/2$ .

### 3. Mixing Length Convection

We follow the model of mixing length convection developed by Grossman, Narayan & Arnett (1993, hereafter GNA) and use their notation, except that we replace the temperature by the isothermal sound speed  $c_s^2 = kT/\mu m_p$ , where  $\mu$  is the dimensionless molecular weight. The properties of convection depend sensitively on the superadiabatic gradient

$$\Delta \nabla c_s^2 = -c_s^2 \frac{d}{dR} \ln \left( \frac{p^{1/\gamma}}{\rho} \right),$$

where  $\gamma$  is the adiabatic index of the gas.

To fix ideas, we consider first a non-rotating gas. The entropy gradient of the gas can be written in terms of  $\Delta \nabla c_s^2$ :

$$T \frac{ds}{dR} = \frac{1}{\gamma-1} \frac{dc_s^2}{dR} - \frac{c_s^2}{\rho} \frac{d\rho}{dR} = -c_p \Delta \nabla c_s^2,$$

where  $c_p = \gamma/(\gamma-1)$  is the specific heat at constant pressure (in units of  $k/\mu m_p$ ). The Brunt-Väisälä frequency  $N$  is given by

$$N^2 = -\frac{1}{\rho} \frac{dp}{dR} \frac{d}{dR} \ln \left( \frac{p^{1/\gamma}}{\rho} \right) = -\frac{g_{eff}}{c_s^2} \Delta \nabla c_s^2,$$

where  $g_{eff} \equiv -(1/\rho)(dp/dR)$  is the radial effective gravity. When  $N^2$  is positive, perturbations in the gas have an oscillatory behavior and the medium is convectively stable. However, when  $N^2$  is negative, i.e. when  $N$  is imaginary, perturbations have a runaway growth, leading to convection. Convection is present whenever  $\Delta \nabla c_s^2$  is positive, i.e. when the entropy decreases outward. This is the well-known Schwarzschild criterion.

We assume that all mixing lengths are equal to a single length  $L_M$ , and we set the dimensionless thermal expansion coefficient to unity (ideal gas). We also ignore the effect of the microscopic viscosity  $\nu$  on the motion of convective eddies. This is not a very safe assumption, but it simplifies the analysis considerably. We believe that it will not affect the qualitative nature of the results. With these assumptions, the various coefficients,  $A, B, D, E$ , in GNA simplify to  $A = D = 0, B = E = (2/L_M)$ .

Borrowing results from GNA, the root mean square turbulent velocity of convective blobs is given by

$$\sigma = \left( \frac{g_{eff} \Delta \nabla c_s^2}{BEc_s^2} \right)^{1/2} = \frac{L_M}{2} (-N^2)^{1/2},$$

and the convective energy flux is

$$F_c = \frac{\rho c_p c_s^2}{g_{eff}} (A + B\sigma)\sigma = -\frac{L_M^2 (-N^2)^{1/2}}{4} \rho T \frac{ds}{dR}.$$

Let us define the effective diffusion constant  $K_c$  for convective energy transport by the relation

$$F_c = -K_c \rho T \frac{ds}{dR}.$$

We then obtain

$$K_c = \frac{L_M^2}{4} (-N^2)^{1/2}. \quad (2)$$

We see that  $K_c$  has an intuitively obvious form; it is the product of  $(-N^2)^{1/2}$ , which describes the characteristic frequency associated with convective motions (more precisely, it is the growth rate of perturbations), and the square of  $L_M$ , the characteristic length scale of convection. The standard treatment of mixing length convection in astrophysics gives a coefficient of  $1/4\sqrt{2}$  rather than  $1/4$  (e.g. Cox & Giuli 1968, Kippenhahn & Weigert 1990). Since empirical estimates of the mixing length make use of the latter coefficient, we incorporate this difference in our definition of the dimensionless mixing length  $l_M$  below.

All mixing lengths are equal in our treatment. It is therefore natural to assume that all transport phenomena in the convective medium have diffusion constants of the same order as equation (2). In this spirit, we assume that the above expression for  $K_c$  is valid also for convective angular momentum transport. Of course, there could be differences in the relative efficiencies of energy and angular momentum transport, associated for instance with different mixing lengths for the two phenomena. As we highlight in this paper, there are large uncertainties even with regard to the sign of the angular momentum flux.

### 3.1. Convection in a Differentially-Rotating ADAF

When there is rotation, new frequencies enter the problem and convection is no longer determined purely by the Brunt-Väisälä frequency  $N$ . In the spirit of our height-integrated approach, let us consider displacements of gas elements in the equatorial plane. In this case, the effective frequency  $N_{eff}$  of convective blobs is given by

$$N_{eff}^2 = N^2 + \kappa^2, \quad (3)$$

where  $\kappa$  is the epicyclic frequency for particle motions in the equatorial plane; for  $\Omega \propto R^{-3/2}$ , we have  $\kappa = \Omega$ . By analogy with equation (2), we may then write the diffusion constant  $K_c$  as

$$K_c = \frac{L_M^2}{4} (-N_{eff}^2)^{1/2}. \quad (4)$$

QG have shown that the restriction to equatorial displacements leads to an underestimate of the growthrate of convective modes. In the Appendix, we present a more general analysis in which we remove the restriction to equatorial displacements. In the rest of the paper, however, we work with equations (3) and (4).

For a self-similar ADAF, we find that

$$N^2 = -\frac{1}{\rho} \frac{dp}{dR} \frac{d}{dR} \ln \left( \frac{p^{1/\gamma}}{\rho} \right) = -\frac{(1+a)[1-(\gamma-1)a]}{\gamma} c_0^2 \Omega_K^2,$$

$$N_{eff}^2 = \left\{ -\frac{(1+a)[(\gamma+1) - (\gamma-1)a]}{\gamma} c_0^2 + 1 \right\} \Omega_K^2.$$

It is not immediately obvious from the above expression whether a given flow will be convectively stable or unstable, since that depends on the sign of  $N_{eff}^2$  which cannot be determined until the full problem is solved and the value of  $c_0^2$  is obtained.

If  $N_{eff}^2 < 0$ , we have a convectively unstable medium and the diffusion constant for energy transport is given by equation (4). Let us write the mixing length  $L_M$  in terms of the pressure scale height:

$$L_M = 2^{-1/4} l_M H_p, \quad H_p = -\frac{dR}{d \ln p} = \frac{R}{(1+a)},$$

where  $l_M$  is the usual dimensionless mixing length parameter (called  $\alpha$  in the solar and stellar convection literature, cf. Kim et al. 1996, Abbett et al. 1997). The additional factor of  $2^{-1/4}$  has been introduced in order to bring our formulae in line with the usual versions of mixing length convection (cf the discussion below eq 2). We also write the diffusion constant in the usual form

$$K_c = \alpha_c \frac{c_s^2}{\Omega_K},$$

where  $\alpha_c$  is a dimensionless coefficient which describes the strength of convective diffusion; this coefficient is similar to the usual Shakura & Sunyaev  $\alpha$  which is used to parameterise the strength of viscosity. We then find that

$$\alpha_c = \frac{l_M^2}{4\sqrt{2}(1+a)^2 c_0^2} \left\{ \frac{(1+a)[(\gamma+1) - (\gamma-1)a]}{\gamma} c_0^2 - 1 \right\}^{1/2}, \quad (5)$$

and the convective energy flux takes the form

$$F_c = -\alpha_c \frac{c_s^2}{\Omega_K} \rho T \frac{ds}{dR}.$$

In the Sun, the mixing length  $l_M$  is estimated to be approximately  $\sim 1.5$  (e.g. Abbett et al. 1997). However, it is believed that  $l_M$  should be smaller when there is a strong superadiabatic gradient (e.g. Kim et al. 1996); for instance, Asida (1999) estimates  $l_M \sim 1.4$  in red giant envelopes. In view of the relatively large superadiabatic gradient present in ADAFs, the convection in these flows is likely to be more similar to that found in red giant envelopes than in the Sun's convection zone. So we may expect  $l_M^2 \sim 2$  in ADAFs. We use this value for numerical estimates, but we note that there is some uncertainty in the estimate.

Transport of angular momentum by convection is a complex subject and there is no consensus on how it operates. We consider two extreme possibilities. In one limit we assume, following NY, that convection behaves like normal viscosity; that is, we write the flux of angular momentum as

$$J_c = -\alpha_c \frac{c_s^2}{\Omega_K} \rho R^3 \frac{d\Omega}{dR}. \quad (6)$$

This corresponds to the assumption that the convective angular momentum flux is oriented down the *angular velocity gradient*, i.e. that convection tries to drive a system towards a state of uniform rotation, just as microscopic viscosity does. For  $\Omega \propto R^{-3/2}$ , it corresponds to outward transport of angular momentum. Equation (6) also assumes that the diffusion constant for angular momentum transport is equal to that for energy transport, hence the use of the same constant  $\alpha_c$ .

An alternative possibility is that the convective flux scales as

$$\dot{J}_c = -\alpha_c \frac{c_s^2}{\Omega_K} \rho R \frac{d(\Omega R^2)}{dR}. \quad (7)$$

This means that the convective angular momentum flux is oriented down the *specific angular momentum gradient*, i.e. that convection tries to drive a system towards a state of uniform specific angular momentum. For  $\Omega \propto R^{-3/2}$ , it corresponds to inward transport of angular momentum.

We concentrate on these two limiting cases in §4 and §5. However, as Kumar, Narayan & Loeb (1995) showed, there could be a continuum of intermediate possibilities, depending on the nature of the interactions between convective eddies. Therefore, we discuss in §6 the general case where the angular momentum flux takes the form

$$\dot{J}_c = -\alpha_c \frac{c_s^2}{\Omega_K} \rho R^{3(1+g)/2} \frac{d[\Omega R^{3(1-g)/2}]}{dR}. \quad (8)$$

Here, the index  $g$  allows us to tune the physics of convective angular momentum transport. When  $g = 1$ , we reproduce equation (6) and when  $g = -1/3$  we reproduce equation (7). In principle, any value of  $g$  between these two extremes is possible. In our problem, the specific case  $g = 0$  corresponds to zero angular momentum transport.

#### 4. Outward Angular Momentum Transfer

We assume that convection moves angular momentum outward according to equation (6). In this case, the only valid self-similar solution is the one found by Narayan & Yi (1994), which has  $a = 3/2$ ,  $\rho \propto R^{-3/2}$ . For this case, we may write the radial velocity as

$$v(R) = v_0 v_K \propto R^{-1/2},$$

where  $v_0$  is a constant.

We consider first the angular momentum equation. We follow Narayan & Yi (1994) and look for a self-similar solution in which the net flux of angular momentum vanishes. This implies that the sum of the angular momentum fluxes due to viscosity  $\dot{J}_v$ , convection  $\dot{J}_c$  and advection  $\dot{J}_{adv}$  is equal to zero. Thus

$$\dot{J} = \dot{J}_v + \dot{J}_c + \dot{J}_{adv} = -(\alpha + \alpha_c) \frac{c_s^2}{\Omega_K} \rho R^3 \frac{d\Omega}{dR} + \rho R v \Omega R^2 = 0,$$

which simplifies to

$$v_0 = -\frac{3}{2}(\alpha + \alpha_c) c_0^2. \quad (9)$$

We consider next the energy equation. Ignoring cooling, but including energy transport by convection, this equation takes the form

$$\rho v T \frac{ds}{dR} + \frac{1}{R^2} \frac{d}{dR} (R^2 F_c) = Q^+.$$

The viscous dissipation rate is equal to (shear stress) × (rate of strain):

$$Q^+ = (\alpha + \alpha_c) \frac{c_s^2}{\Omega_K} \rho R^2 \left( \frac{d\Omega}{dR} \right)^2.$$

Substituting equation (1) for  $\Omega_0$  and equation (8) for  $v_0$ , and simplifying, this reduces to the following relation,

$$\left[ \frac{(5-3\gamma)}{(\gamma-1)}(3\alpha + \alpha_c) + \frac{45}{2}(\alpha + \alpha_c) \right] c_0^2 = 9(\alpha + \alpha_c), \quad (10)$$

where we recall that  $\alpha_c$  is itself a function of  $c_0^2$  (cf. eq. 5). We note that equation (10) is equivalent to equation (36) in Kato & Nakamura (1998). Given the values of  $\alpha$  and  $\gamma$ , this equation may be solved for  $c_0^2$ . Equations (1) and (9) then allow us to calculate the angular velocity and radial velocity, thus completing the solution.

The solid lines in Fig. 1 show the variation of the convective coefficient  $\alpha_c$  as a function of the viscous coefficient  $\alpha$  for three choices of  $\gamma$ : 1.6, 1.5, 1.4. We see that  $\alpha_c$  lies in the range 0.02 to 0.07, depending on the values of  $\alpha$  and  $\gamma$ . The estimate of  $\alpha_c$  is directly proportional to  $l_M^2$ , which we have set equal to 2.

An important result of this analysis is that we obtain a consistent solution for all values of  $\alpha$  and for any  $\gamma < 5/3$ . In other words, the NY self-similar solution, with  $a = 3/2$ , is valid in the presence of convection for all values of  $\alpha$ , provided convection transfers angular momentum outward with the same efficiency as it transfers energy (i.e. same  $\alpha_c$ ). This result was already obtained by NY using a somewhat simplified model of convection. We have presented here a more detailed analysis, using a slightly more rigorous version of mixing length convection.

Note that for the NY self-similar solution the value  $\gamma = 5/3$  is special. For  $\gamma = 5/3$  and any value of  $\alpha$ , we find  $c_0^2 = 2/5$ ,  $\Omega_0^2 = 0$  (no rotation) and  $\alpha_c = 0$  (no convection). There are no self-similar solutions of the NY form for  $\gamma > 5/3$ .

## 5. Inward Angular Momentum Transfer

We now consider the case when angular momentum is moved inward by convection, following the prescription given in equation (7). To our knowledge, this case has not been considered previously in the theory of ADAFs.

### 5.1. Self-Similar ADAF Solution

We consider first the case when  $a = 3/2$ . The analysis proceeds very similarly as in the previous section. The angular momentum equation looks the same as before, except that  $\dot{J}_c$  is now proportional to  $-d(\Omega R^2)/dR$  rather than  $-d\Omega/dR$ . Correspondingly, the vanishing of the angular momentum flux gives the following condition:

$$v_0 = -\frac{1}{2}(3\alpha - \alpha_c)c_0^2. \quad (11)$$

In the energy equation, we note that the net viscous stress, including the effect of viscosity, is now proportional to  $(3\alpha - \alpha_c)/2$ . We once again write  $Q^+$  as (shear stress)  $\times$  (rate of strain). Then, instead of equation (10), we obtain the following relation,

$$\frac{(5-3\gamma)}{(\gamma-1)}(\alpha - \alpha_c)c_0^2 = (3\alpha - \alpha_c) \left( 1 - \frac{5}{2}c_0^2 \right), \quad (12)$$

where once again  $\alpha_c$  is a function of  $c_0^2$ .

The solid lines on the right in Figure 2 show the variation of  $\alpha_c$  with  $\alpha$  for various values of  $\gamma$ . As before, we see that  $\alpha_c$  lies in the range  $\sim 0.02 - 0.07$ . However, we now find that a consistent solution is available only for  $\alpha$  greater than a certain critical  $\alpha_{crit1}$ , whose value lies in the range 0.03 to 0.08. The value of  $\alpha_{crit1}$  depends on the value of  $\gamma$ , and is also directly proportional to  $l_M^2$ .

When  $\alpha = \alpha_{crit1}$ , the sound speed takes on its maximum value,  $c_0^2 = 2/5$  (and the rotation goes to zero, cf. eq 1). Knowing this fact, it is straightforward to show that

$$\alpha_{crit1} = \alpha_{c,crit1} = \frac{l_M^2}{20} \left( \frac{5 - 3\gamma}{\gamma} \right)^{1/2},$$

where  $\alpha_{c,crit1}$  is the value of the convective  $\alpha_c$  when  $\alpha = \alpha_{crit1}$ . Note once again that the solution is valid only for  $\gamma \leq 5/3$ .

## 5.2. Self-Similar Convective Envelope Solution

What happens if  $\alpha < \alpha_{crit1}$ ? In this case, there is no NY-like self-similar solution with  $a = 3/2$ . A possible reason for the lack of solution is the following. Since advection moves angular momentum inward and since we have assumed (in this section) that convection also moves angular momentum inward, the only way to have a consistent self-similar accretion solution is for  $\alpha$  viscosity to move an equivalent amount of angular momentum outward. If the parameter  $\alpha$  is very small, the viscous flux is unable to cope with the inward flux due to convection, and there is no consistent accretion solution.

However, we find that when  $\alpha$  is small, a completely different solution, with  $a = 1/2$ ,  $\rho \propto R^{-1/2}$ , is possible. This is a *non-accreting* solution with  $v = 0$  (at least in the limit of perfect self-similarity). We refer to it as a “convective envelope” solution, or a “convection-dominated accretion flow” (QG).

Since  $v = 0$  in this solution, the advected angular momentum flux  $\dot{J}_{adv}$  vanishes. Therefore, we must have  $\dot{J}_v + \dot{J}_c = 0$ , i.e. there must be a perfect balance between outward angular momentum transport via viscosity and inward transport via convection. This leads to the following condition on  $c_0^2$ :

$$\alpha = \frac{1}{3}\alpha_c = \frac{l_M^2}{27\sqrt{2}c_0^2} \left\{ \frac{3(\gamma + 3)}{4\gamma} c_0^2 - 1 \right\}^{1/2}. \quad (13)$$

If  $\alpha$  is very small, then  $\alpha_c$  is also very small. In this limit, we have a flow which is marginally stable to convection, with  $c_0^2 = 4\gamma/3(\gamma + 3)$ . (This result is valid only if we restrict the analysis to equatorial motions; see the Appendix for a more general discussion.)

The convective envelope solution satisfies the energy equation trivially. Since the net angular momentum flux vanishes, there is no shear stress, and  $Q^+ = 0$ . Furthermore, since  $v = 0$ , there is no advection of entropy. Finally, since  $a = 1/2$ , the convective energy flux  $F_c \propto R^{-2}$  and therefore the divergence of convective energy flux vanishes. This last property, which is essential in order to satisfy the energy equation, is what fixes  $a = 1/2$  for the solution.

Equation (13) allows us to solve for  $\alpha_c$  as a function of  $\alpha$  and  $\gamma$ . The solid line segments on the left in Fig. 2 show the results. Interestingly, we find that there is a consistent solution only if  $\alpha$  is less than a critical  $\alpha_{crit2}$ . The critical value is obtained by setting  $c_0^2$  equal to the largest value it is allowed for  $a = 1/2$ , viz.  $2/3$  (see eq 1). This gives

$$\alpha_{crit2} = \frac{1}{3}\alpha_{c,crit2} = \frac{l_M^2}{36} \left( \frac{3 - \gamma}{\gamma} \right)^{1/2}.$$



We see that  $\alpha_{crit2}$  is of the same order as  $\alpha_{crit1}$ , i.e.  $\sim 0.05$ , but that the two are not exactly equal. An interesting feature is that  $\gamma = 5/3$  is not special for this solution. Consistent flows can be obtained even for larger  $\gamma$ .

Note that a convection-dominated accretion flow is technically not an accretion flow at all, but a static configuration. In practice of course, a small amount of mass will flow into the central black hole from the innermost region and this will drive a small amount of accretion. However, in contrast to the ADAF solution described by NY, where the mass accretion rate is determined by the density and temperature on the outside and is not sensitive to the radius of the inner boundary, in the convective envelope the accretion rate is determined entirely by the conditions at the inner boundary and therefore on the location of the inner boundary.

Another interesting feature is that the convective envelope solution has a significant outward flux of energy carried by convection. This energy flux is constant with radius and clearly originates near the center. Indeed, the flux originates from the (small amount of) mass which is accreted at the inner edge. A fraction of the binding energy of this accreted mass is diverted outward by convection and is transported to large radii, where it is presumably radiated in some fashion. This feature of the convective envelope solution, namely that energy which is generated deep in the center is transported a large distance radially before being radiated, is very similar to what happens in the convection zone of low-mass main-sequence stars like the Sun and red giants.

## 6. General Angular Momentum Transfer

For completeness, we briefly discuss the general case in which the angular momentum transfer is described by equation (8) with an arbitrary index  $g$ .

If we consider an NY-like self-similar solution with  $a = 3/2$ , equations (10) and (12) are replaced by the more general relation

$$\left[ \frac{3(5-3\gamma)}{(\gamma-1)} c_0^2 + \frac{45}{2} c_0^2 - 9 \right] \alpha = \left[ 9g - \frac{(3g-2)(5-3\gamma)}{(\gamma-1)} c_0^2 - \frac{45g}{2} c_0^2 \right] \alpha_c,$$

where  $\alpha_c$  is still given by equation (5). It is easily verified that this equation reduces to equation (10) for  $g = 1$  and equation (12) for  $g = -1/3$ . We can also show that the critical  $\alpha_{crit1}$  becomes

$$\alpha_{crit1} = \left( \frac{2}{3} - g \right) \alpha_{c,crit1} = \left( \frac{2}{3} - g \right) \frac{l_M^2}{20} \left( \frac{5-3\gamma}{\gamma} \right)^{1/2}.$$

We see that  $\alpha_{crit1}$  is positive whenever  $g < 2/3$ . This is an interesting result. It shows that the breakdown of the NY solution at small  $\alpha$  is not unique to the prescription (7) for the angular momentum transfer, which corresponds to  $g = -1/3$ . The same thing happens even when there is no angular momentum transfer by convection ( $g = 0$ ) or when there is angular momentum transfer outward but with a reduced efficiency compared to equation (6) ( $0 < g < 2/3$ ). In these cases, the critical  $\alpha_{crit1}$  is smaller than when  $g = -1/3$ , which means that  $\alpha$  has to be lower before the NY solution would fail.

Similarly, when we repeat the analysis of §5.2 that led to the convective envelope solution, we find for a general value of  $g$  that equation (13) is replaced by

$$\alpha = -g\alpha_c = -\frac{gl_M^2}{9\sqrt{2}c_0^2} \left\{ \frac{3(\gamma+3)}{4\gamma} c_0^2 - 1 \right\}^{1/2}.$$

We see that the convective envelope solution is allowed for any  $g < 0$ , but not for  $g > 0$ . The critical  $\alpha_{crit2}$  up to which the solution is available is

$$\alpha_{crit2} = -g\alpha_{c,crit2} = -\frac{gl_M^2}{12} \left( \frac{3-\gamma}{\gamma} \right)^{1/2}.$$

One interesting fact that emerges from this analysis (as well as the simpler version presented in §5) is that there are certain parameter regimes for which neither an NY-like self-similar solution nor a convective envelope solution is possible. Any flow with  $0 < g < 2/3$  and  $\alpha < \alpha_{crit1}$  belongs to this category. For this parameter range, power-law solutions, if any, would violate one of our basic assumptions. The most likely modification is the scaling  $\Omega \propto \Omega_K \propto R^{-3/2}$  which we have assumed. Honma (1996), for instance, discovered an ADAF solution for  $\gamma = 5/3$  which has  $\Omega \propto R^{-1/2}$ . This solution has been developed further by Kato & Nakamura (1998) and Manmoto et al. (2000).

## 7. Comparison with Numerical Simulations

In this section we compare the theory developed in the previous section with numerical results from a low-viscosity two-dimensional (2D) simulation of a non-radiative accretion flow. The model was calculated by solving the non-relativistic time-dependent Navier-Stokes equations for an accretion flow in the gravitational field of a point mass. All components of the viscous stress were included. The details of the numerical technique are described in Igumenshchev & Abramowicz (1999).

The model considered here has  $\alpha = 0.01$ ,  $\gamma = 5/3$ , inner boundary of the accretion flow at  $R_{in} = 3R_g$  and outer boundary at  $R_{out} = 8 \times 10^3 R_g$ , where  $R_g$  is the gravitational radius of the black hole. Mass is steadily injected within an equatorial torus near the outer boundary of the grid. There is no cooling in the accreting gas.

Initially, there is little or no mass in the grid. As the injected mass spreads and accretes, the mass within the grid increases. After a period of time comparable to the viscous time scale at the outer radius, the accretion flow achieves a quasi-stationary behaviour, and may be considered to be in steady state. The “steady state” is, however, only in a time-averaged sense since the flow has convective motions which introduce chaotic fluctuations at any given point. We compute time-averaged properties of the flow for comparison with the theoretical predictions by averaging over a time equal to 44 Keplerian periods measured at  $100R_g$ .

Before we describe the results we would like to emphasize an important point. Stone & Balbus (1996) showed that if azimuthal pressure gradients are absent, then turbulence in a Keplerian disk can only transport angular momentum inward. By symmetry, 2D axisymmetric simulations do not have azimuthal pressure gradients. Because of this, each eddy preserves its angular momentum as it moves (in the absence of ordinary viscosity). Therefore, turbulent mixing of eddies in axisymmetric simulations tends to drive the system towards a state of constant specific angular momentum, and the transfer of angular momentum behaves like equation (7). We emphasize that this is merely a consequence of axisymmetry, and does not necessarily represent the properties of real convection.

Our numerical simulations confirm the above expectation for the direction of transfer of angular momentum. Figure 3 shows the  $(R, \phi)$ -component of the Reynolds stress  $\sigma_{R\phi} \equiv \langle \rho v'_R v'_\phi \rangle$  as a function of radius,

where the stress has been averaged over polar angle  $\theta$  as follows:

$$\sigma_{R\phi}(R) = \frac{\int_0^\pi \sigma_{R\phi}(R, \theta) \sin \theta d\theta}{\int_0^\pi \rho(R, \theta) \sin \theta d\theta}.$$

We see that, except near the boundaries ( $R < 5R_g$  and  $R > 10^3R_g$ ), the Reynolds stress is negative everywhere in the flow. This indicates that the bulk convective motions in the gas move angular momentum inward. Equating the numerical estimate of  $\sigma_{R\phi}$  and the convective stress  $K_c\rho(\partial\Omega R^2/\partial R)/R$ , we obtain an estimate  $\alpha_c \simeq 3\langle v'_R v'_\phi \rangle / v_K^2 = 10^{-2}$ , where we have used  $H/R = 1/2$ . Thus,  $\alpha_c/\alpha \simeq 1$  in the numerical model.

Because the convective angular momentum transfer in the simulation follows equation (7), we must make use of the analysis presented in §5 for interpreting the numerical results. Moreover, since  $\alpha$  is very small ( $\alpha = 0.01$ ), we expect the simulation to reproduce the low- $\alpha$  convective envelope solution with  $\rho \propto R^{-1/2}$  rather than the high- $\alpha$  NY branch of solution. To test this prediction, we show in Fig. 4 the profiles of  $\rho$ ,  $c_s^2/v_K^2$ ,  $|v|/v_K$  and  $\Omega/\Omega_K$  as functions of  $R$ . Each quantity has been averaged over  $\theta$  exactly as in the case of the Reynolds stress.

The simulation gives a density profile with  $\rho \propto R^{-1/2}$ , as expected from the theory. A similar  $R^{-1/2}$  variation was seen also in low-viscosity ADAF simulations by Igumenshchev & Abramowicz (1999) and by Stone et al. (1999). The latter authors considered a variety of viscosity prescriptions, of which Run K corresponded to the usual  $\alpha$  prescription; this run exhibited  $\rho \propto R^{-1/2}$  behavior, as expected for the convective envelope. It may be worth emphasizing that the  $R^{-1/2}$  density profile in the convective envelope solution (which is very different from the  $R^{-3/2}$  profile of the self-similar NY solution) is not a consequence of mass loss. In the analytic work presented in this paper, for instance, we explicitly assume that there is no mass loss. Both Igumenshchev & Abramowicz (1999) and Stone et al. (1999) found that for low values of  $\alpha$  there were no powerful unbound outflows in their numerical simulations.

In this context, note that because the medium is convectively turbulent and is not accreting, roughly half the mass at any radius at any given time will be flowing in and half will be flowing out. We could estimate a “mass inflow rate”  $\dot{M}_{in}(R)$  by adding up all the inflowing gas elements. This would give  $\dot{M}_{in} \sim 4\pi\rho\sigma RH/2$  where  $\sigma$  is the root mean square velocity of the turbulent eddies. In §3 we showed that  $\sigma$  scales as  $L_M(-N_{eff}^2)^{1/2} \sim v_K \sim R^{-1/2}$ . Therefore, for  $\rho \propto R^{-1/2}$  and  $H \propto R$ , we find that  $\dot{M}_{in} \propto R$ . It might be tempting to identify the rapid decline of  $\dot{M}_{in}$  with decreasing radius as evidence for a massive outflow. But there is no reason to think that the outflowing gas at any radius in the interior of the flow will escape and flow out to infinity. It is more than likely that the outflowing gas forms part of convective eddies, so that the mass that is flowing out at a certain time will later turn around and flow in. If such is the case, then the quantity  $\dot{M}_{in}$  is not very useful.

The analytic convective envelope solution predicts that  $\dot{M} = 0$  and  $v = 0$ . As Fig. 4 shows, the mean radial velocity in the simulation is extremely small, but it is not exactly zero. The small non-zero value is because the simulated flow has an inner boundary where some mass can flow into the black hole. Thus there is a small  $\dot{M}$  which leads to a finite  $v$ . The scalings discussed in §2 show that for  $\rho \propto R^{-1/2}$ , we expect the velocity to scale as  $v \propto v_K/R$ . This is confirmed in Fig. 4.

The profiles of  $c_s^2(R)$  and  $\Omega(R)$  in Fig. 4 show the predicted power-law behaviors of these quantities for  $10R_g < R < 10^3R_g$ . However, a comparison of actual numerical values does not give good agreement. From

equations (1) and (13), for  $a = 1/2$ ,  $\gamma = 5/3$  and very small  $\alpha$ , the theory predicts

$$\frac{c_s^2}{v_K^2} = \frac{4\gamma}{3(3+\gamma)} = 0.48, \quad \frac{\Omega}{\Omega_K} = \left(\frac{3-\gamma}{3+\gamma}\right)^{1/2} = 0.53.$$

The numerical simulations give  $c_s^2/v_K^2 = 0.26$  and  $\Omega/\Omega_K = 0.9$ . As QG have shown, this discrepancy is the result of the height-integrated approximation. We discuss in the Appendix an improved theory that avoids this approximation. The theory predicts  $c_s^2/v_K^2 = 0.29$  and  $\Omega/\Omega_K = 0.75$ , in better agreement with the simulations.

An important feature of the convective envelope solution is that there is a strong outward flux of energy  $F_c$  transported by convection. The corresponding luminosity is equal to  $\dot{E}_c = 4\pi R H F_c$ , which is independent of radius. Comparison of the theoretical estimate with numerical results from the simulation show quite good agreement. Substituting the numerical value of  $\rho R^{1/2}$  at  $R = 100R_g$  in the analytical expression for  $F_c$ , we estimate  $\dot{E}_c \simeq 0.2\alpha_c$  in units of  $\dot{M}c^2$ , where  $\dot{M}$  is the mass accretion rate into the black hole. On the other hand, the numerical simulations give  $\dot{E}_c = \dot{E}_{tot} - \dot{E}_v \simeq 2 \times 10^{-3}$ , where  $\dot{E}_{tot}$  is the total outward energy flux and  $\dot{E}_v$  is the energy flux due to viscosity. Equating the two estimates of the convective flux we get  $\alpha_c \simeq 10^{-2}$ . This estimate of  $\alpha_c$  agrees with our previous estimate from the Reynolds stress, which is encouraging considering the uncertainties (physical and numerical) of the two estimates. Thus, we feel that the convective envelope model is a good description of numerically simulated 2D ADAFs at low  $\alpha$ .

## 8. Discussion

The main result of this paper is that, in addition to the NY self-similar ADAF solution which has density  $\rho \propto R^{-3/2}$ , there is a second power-law solution, a radiatively inefficient “convective envelope” solution or “convection-dominated accretion flow,” in which  $\rho \propto R^{-1/2}$ . The second solution corresponds to a static envelope in which the mass accretion rate is very small. Indeed,  $\dot{M}$  vanishes in the limit when the inner edge of the accretion flow moves down to 0. The solution has well-developed convection and is perfectly balanced in the sense that it transfers as much angular momentum outward via viscosity as it transports inward via convection. There is, however, a net outward flux of energy.

The convective envelope solution is possible only when two conditions are simultaneously met:

- (i) The viscosity coefficient  $\alpha$  must be fairly small. For a reasonable choice of the mixing length parameter ( $l_M^2 \sim 2$ ), we find that we require  $\alpha < \alpha_{crit2} \sim 0.05$  (see Fig. 2). The improved analysis presented in the Appendix modifies the value upward.
- (ii) Convection must transport angular momentum inward ( $g = -1/3$ , §5) or not transport angular momentum at all ( $g = 0$ , §6). If it transports angular momentum outward, it must do so with less efficiency than it transports energy; specifically, we require  $g < 2/3$  (§6).

The numerical simulations discussed in §7 and in Igumenshchev & Abramowicz (1999) and Stone et al. (1999) satisfy both of the above conditions. In particular, condition (ii) is automatically satisfied by all numerical simulations of ADAFs carried out so far since all these simulations have been axisymmetric. The axisymmetry guarantees that there are no azimuthal pressure gradients and so convective eddies transport angular momentum inward (Stone & Balbus 1996). We find that the numerical results agree quite well with the analytical results (Figs. 3, 4, §7).

In all cases where either condition 1 or 2 is violated, the only self-similar solution we have been able to

find is the solution derived by NY, in which  $\rho \propto R^{-3/2}$ . For given outer boundary conditions, this solution leads to a considerably larger mass accretion rate than that obtained with the convective envelope solution.

Igumenshchev & Abramowicz (1999) found that convection plays a negligible role when  $\alpha$  is  $\gtrsim 0.1$ . This is consistent with our analysis, which shows that the convective  $\alpha_c$  is much less than  $\alpha$  in this regime (Figs. 1, 2). Indeed, our analysis overestimates  $\alpha_c$  for such models because the mixing length formalism we employ is a local steady state theory which assumes that convection has achieved saturation amplitude. However, the convective turnover time, which is given by  $t_{conv} = (-N_{eff}^2)^{-1/2}$  is of order  $1/\alpha_c\Omega_K$ , whereas the accretion time in the NY solution is of order  $t_{acc} \sim 1/\alpha\Omega_K$ . Thus  $t_{conv}/t_{acc} \sim \alpha/\alpha_c$ , and this becomes large as  $\alpha$  increases. The net effect would be to reduce  $\alpha_c$  below the values shown in Figs. 1 and 2. Thus, we expect convective motions to be negligibly small for  $\alpha \gtrsim 0.1$ , as confirmed by Igumenshchev & Abramowicz (1999). (Stone et al. 1999 did not explore models with such large values of  $\alpha$ .)

The range  $\alpha \sim 0.1 - 0.3$  is found to be very interesting in Igumenshchev & Abramowicz’s (1999) simulations. For  $\alpha = 0.3$ ,  $\gamma = 1.5$ , they found that there is a pure inflow, while for other choices, e.g.  $\alpha = 1$ ,  $\gamma = 1.5$ , they obtained a stable bipolar outflow. Igumenshchev (2000) studied a model with  $\alpha = 0.1$ ,  $\gamma = 5/3$  and found a global meridional circulation pattern accompanied by a surprising *unipolar* supersonic outflow. The flow has some resemblance to the convective envelope solution discussed in this paper. Only a small fraction of the circulating matter is directly accreted by the black hole, and the energy required to support the circulation is extracted from the infalling mass with an efficiency  $\sim 10^{-3} - 10^{-2}$ . The circulation transports the energy to large radii, where the author argues it could be radiated via bremsstrahlung. It would appear that in this model, viscosity is large enough to suppress convection on scales  $\lesssim R$ , but global circulation on a scale  $\sim R$  still survives, and this transports energy.

The parallel between this solution and our convective envelope solution is fairly strong. The convective envelope again converts a fraction of the binding energy of the accreting mass into an outward flux of energy, which is carried by convection. This energy somehow has to be got rid of at the outer boundary. One way in which the energy could be eliminated from the system is by driving a slow (but perhaps massive) outflow from the outer boundary. Another is that the energy could be radiated by gas on the outside, as suggested by Igumenshchev (2000).

The latter is quite plausible. Since  $\rho \propto R^{-1/2}$  and  $T \propto R^{-1}$ , the bremsstrahlung cooling rate per unit volume varies as  $Q_{brems}^- \propto \rho^2 T^{1/2} \propto R^{-3/2}$ . The cooling time scale thus goes as  $t_{cool} \propto \rho T / Q_{brems}^- \propto R^0$ . In comparison, since  $v \propto R^{-3/2}$ , the accretion time scale goes as  $t_{acc} = R/v \propto R^{5/2}$ , and the ratio  $t_{acc}/t_{cool} \propto R^{5/2}$  increases very rapidly with radius. Therefore, one naturally expects a highly advection-dominated convection zone (presumably well described by our convective envelope solution) sandwiched between an inner energy producing zone close to the black hole and an outer radiating zone. The radiating zone would have very specific spectral signatures which would be interesting to explore.

Is the convective envelope solution relevant for real accretion flows? This depends on the answers to two questions.

The first question is: What is the value of  $\alpha$  in real ADAFs? If  $\alpha > \alpha_{crit2} \sim 0.05$ , then the convective envelope solution is not possible and the second question below is irrelevant. Empirical estimates of  $\alpha$  from fitting the spectra of black hole systems suggest that  $\alpha$  is large. Narayan (1996) obtained  $\alpha \sim 1$ , which Esin, McClintock & Narayan (1997) later revised to  $\alpha \sim 0.2 - 0.3$ . Quataert & Narayan (1999) considered models with  $\alpha = 0.1$ , but they did not verify that such low values of  $\alpha$  are consistent with the constraints that Narayan (1996) and Esin et al. (1997) considered, specifically the existence of luminous black hole X-ray binaries in the “low” spectral state. More work is needed before one can state with confidence whether or

not values of  $\alpha \lesssim \alpha_{crit2}$  are consistent with observations.

On the theoretical front, although there is good reason to believe that “viscosity” in differentially-rotating accretion flows is produced by magnetic stresses generated by the Balbus & Hawley (1992, 1998) instability, the theory has not developed to the point where the value of  $\alpha$  can be estimated. Numerical MHD simulations give values over a wide range,  $\alpha \lesssim 0.01$  to  $\alpha \sim 0.6$  (Balbus & Hawley 1998). Furthermore, all simulations so far have been done on thin accretion disks, and it is unclear whether those results are valid for the much thicker ADAFs. Numerical MHD simulations of accretion flows under ADAF-like conditions would be very worthwhile. The simulations will need to be done in three dimensions rather than two, since even in the thin disk case, there are large differences between 2D and 3D simulations (Balbus & Hawley 1998).

The second question is: Does convection in differentially-rotating ADAFs move angular momentum outward or inward?

Ryu & Goodman (1992) showed that linear modes in a convectively unstable thin accretion disk transfer angular momentum inward. Stone & Balbus (1996) used numerical simulations to study the non-linear version of the problem. They found that angular momentum was either transported very weakly inward or not at all. These are significant results, but their relevance to ADAFs is a little uncertain. As NY emphasized, the entropy gradient in a thin disk model is in the vertical direction whereas the angular momentum gradient is in the horizontal direction. In ADAFs on the other hand, both the entropy gradient and the angular velocity/angular momentum gradient are in the radial direction. This might conceivably cause some differences in the physics.

Kumar, Narayan & Loeb (1995) analysed convective angular momentum transport in a differentially rotating medium using a mixing length formalism. They found that, while small amplitude linear perturbations transport angular momentum down the specific angular momentum gradient, in agreement with the result of Ryu & Goodman (1992), nonlinear saturated convection generally behaves very differently. Indeed, in the nonlinear regime, the angular momentum transport depends critically on the nature of the interactions between convective eddies, which Kumar et al. modeled via a scattering term. By tuning their scattering function, they could reproduce a wide variety of behaviors, covering the entire range from  $g = -1/3$  to  $g > 1$  (in the language of the present paper).

Stone & Balbus (1996) analyzed the basic hydrodynamic equations in a turbulent Keplerian disk and showed that, when azimuthal pressure perturbations are small, there can be no net outward transport of angular momentum. As already mentioned, this powerful result is the reason why axisymmetric numerical simulations of convecting disks always move angular momentum inward. It also throws considerable light on the Kumar et al. (1995) work since the eddy scattering function invoked by these authors implicitly involves azimuthal pressure fluctuations. It is the scattering that enables their model to transport angular momentum outward.

Despite these theoretical studies, the basic question of how angular momentum transport actually operates in a convection-dominated accretion flow remains very much open. Specifically, it is unclear how important azimuthal pressure perturbations are in these systems, and whether angular momentum is transported outward or inward. We see only one way to answer this question: full three-dimensional numerical simulations. If 3D simulations are too expensive, one should at least carry out nonaxisymmetric two-dimensional simulations in cylindrical geometry.

One empirical fact is worth noting; the convection zone in the Sun is closer to being in a state of constant

angular velocity than a state of constant angular momentum. Indeed, in the equatorial plane, the angular velocity actually increases with increasing radius, which motivated Kumar et al. (1995) to consider models with  $g > 1$ . One of the two conditions, (i) and (ii), mentioned at the beginning of this section must be violated in the Sun. One possibility is that the effective viscous  $\alpha$  in the Sun is large enough to counter any inward transport of angular momentum by convection. This is reasonable since the convective motions in the Sun are not very energetic, and  $\alpha$  does not have to be very large to counter the effect of convection. Alternatively, perhaps convection in the Sun behaves as in equation (6) and drives the system to near-zero  $d\Omega/dR$ . The Sun is certainly not a good comparison for an ADAF — a more rapidly rotating convective star would be closer. Nevertheless, the fact that the Sun has achieved an equilibrium configuration that is very different from a constant specific angular momentum state must be treated as a possible clue as we grope towards a better understanding of advection-dominated flows.

In closing, we note that the key point of this paper is that there is considerable uncertainty associated with angular momentum transport by convection, and that this leads to two very distinct configurations for an ADAF. There is a related, though less uncertain, issue connected to energy transport. We considered in this paper convective transport, where energy is transported down the entropy gradient. In addition, there could also be conduction which transports energy down the temperature gradient. Conduction has been studied by Gruzinov (1999) in the context of Bondi accretion. It would be of interest to extend Gruzinov’s analysis to ADAFs and to investigate models in which convection and conduction are both present in an accretion flow.

*Acknowledgments.* The authors thank Eliot Quataert and Andrei Gruzinov for sharing their results prior to publication and for permitting use of some of their methods, the referee, Mitch Begelman, for useful comments, and SISSA (Trieste, Italy) for hospitality while this work was done. RN thanks Dimitar Sasselov for guidance on the mixing length parameter  $l_M$ . This work was supported in part by NSF grants PHY 9507695 and AST 9820686, and the Royal Swedish Academy of Sciences.

## References

- Abbett, W., Beaver, M., Davids, B., Georgobiani, D., Rathbun, P., & Stein, R. 1997, ApJ, 480, 395  
Abramowicz, M., Chen, X., Kato, S., Lasota, J.-P., & Regev, O., 1995, ApJ, 438, L37  
Abramowicz, M., Czerny, B., Lasota, J. P., & Szuszkiewicz, E. 1988, ApJ, 332, 646  
Asida, S. M. 1999, ApJ, in press (astro-ph/9907446)  
Balbus, S. A., & Hawley, J. F. 1992, ApJ, 400, 610  
Balbus, S. A., & Hawley, J. F. 1998, RMP, 70, 1  
Begelman, M. C., & Meier, D. L. 1982, MNRAS, 253, 873  
Blandford, R. D., & Begelman, M. C., 1999, MNRAS, 303, L1  
Chen, X., Abramowicz, M. A., Lasota, J. P., Narayan, R., & Yi, I. 1995, ApJ, 443, L61  
Cox, J. P., & Giuli, R. T. 1968, Principles of Stellar Structure (New York: Gordon & Breach)  
Esin, A. A., McClintock, J. E., & Narayan, R. 1997, ApJ, 489, 865  
Grossman, S. A., Narayan, R., & Arnett, D. 1993, ApJ, 407, 284 (GNA)  
Gruzinov, A. 1999, ApJ, submitted (astro-ph/9809265)  
Honma, F. 1996, PASJ, 48, 77  
Ichimaru, S. 1977, ApJ, 214, 840  
Igumenshchev, I. V., Chen, X., & Abramowicz, M. A. 1996, MNRAS, 278, 236  
Igumenshchev, I. V., & Abramowicz, M. A. 1999, MNRAS, 303, 309  
Igumenshchev, I. V. 2000, MNRAS, in press (astro-ph/9912170)  
Kato, S., Fukue, J., & Mineshige, S. 1998, Black-Hole Accretion Disks (Kyoto: Kyoto Univ. Press)  
Kato, S., & Nakamura, K. E. 1998, PASJ, 50, 559  
Kim, Y.-C., Fox, P., Demarque, P., & Sofia, S. 1996, ApJ, 461, 499  
Kippenhahn, R., & Weigert, A. 1990 Stellar Structure and Evolution (New York: Springer)  
Kumar, P., Narayan, R., & Loeb, A. 1995, ApJ, 453, 480

- Manmoto, T., Kato, S., Nakamura, K. E., & Narayan, R. 2000, ApJ, in press
- Narayan, R. 1996, ApJ, 462, 136
- Narayan, R., Mahadevan, R., & Quataert, E. 1998, in Theory of Black Hole Accretion disks, eds. M. A. Abramowicz, G. Bjornsson, & J. E. Pringle (Cambridge Univ. Press), p148
- Narayan, R., & Yi, I. 1994, ApJ, 428, L13 (NY)
- Narayan, R., & Yi, I. 1995a, ApJ, 444, 231
- Narayan, R., & Yi, I. 1995b, ApJ, 452, 710
- Quataert, E., & Gruzinov, A. 2000, ApJ, submitted (QG, astro-ph/9912440)
- Quataert, E., & Narayan, R. 1999, ApJ, 520, 298
- Ryu, D., & Goodman, J. 1992, ApJ, 388, 438
- Stone, J. M., & Balbus, S. A. 1996, ApJ, 464, 364
- Stone, J. M., Pringle, J. E., & Begelman, M. C. 1999, MNRAS, 310, 1002
- Tassoul, J.-L. 1978, Theory of Rotating Stars, Princeton Univ. Press



### Appendix A

The model of convection which we employed in the main text of the paper is somewhat limited because of our use of height-integrated equations. In particular, when we calculated the diffusion constant associated with convection, we set the characteristic growthrate of convective motions equal to  $(-N_{eff}^2)^{1/2}$ , where  $N_{eff}^2 = N^2 + \kappa^2$ , and  $N$  is the Brunt-Väisälä frequency and  $\kappa = \Omega$  is the epicyclic frequency (see eqs 3 and 4). This is appropriate for a one-dimensional flow in which convective blobs experience displacements only in the equatorial plane. However, as QG have pointed out and as is well-known for rotating fluids (e.g. Tassoul 1978, Begelman & Meier 1982), in the full 2D flow the most unstable modes are not in the equatorial plane. In this Appendix we present a modified analysis in which we identify the most unstable mode and use its properties to estimate the effects of convection. We draw heavily on the work of QG (specifically, the Appendix of their paper).

We consider an axisymmetric self-similar 2D flow in polar coordinates:  $r\theta$ . We assume that the density varies as  $r^{-a}$  (QG use  $n$  instead of  $a$ ) and that the azimuthal velocity  $v_\phi$  and the sound speed  $c_s$  vary as  $r^{-1/2}$ . Using QG's results as a guide, we assume that  $v_\phi$  and  $c_s$  at a given  $r$  are both independent of  $\theta$ . (QG showed this only for the convectively marginally stable system, but we assume that the result is valid also for the more general situation we consider.) In terms of the Keplerian velocity  $v_K = (GM/r)^{1/2}$ , we may write

$$v_\phi(r, \theta) = \Omega_0 v_K(r). \quad (A1)$$

Consider a blob of material at some arbitrary  $r\theta$  and imagine imposing a unit displacement:  $dr = \cos \chi$ ,  $r d\theta = \sin \chi$ . Following the analysis presented by QG, the effective frequency  $N_{eff}$  associated with the dynamics of the blob is given by

$$-\frac{\gamma N_{eff}^2}{\Omega_K^2} = A \cos^2 \chi + B \sin^2 \chi + C \cos \chi \sin \chi, \quad (A2)$$

where the quantities  $A$ ,  $B$  and  $C$  are (we have translated the expressions given in QG to the notation of this paper):

$$A = 1 - a(\gamma - 1) + [a(\gamma - 1) - (\gamma + 1)]\Omega_0^2, \quad (A3)$$

$$B = -\frac{(a+1)(\gamma-1)\cot^2\theta\Omega_0^4}{(1-\Omega_0^2)} - 2\gamma\cot^2\theta\Omega_0^2, \quad (A4)$$

$$C = 2[a(\gamma-1) - (\gamma+1)]\cot\theta\Omega_0^2. \quad (A5)$$

QG show that there are additional terms in  $B$  and  $C$  which depend on  $dv_\phi/d\theta$ , but these terms vanish under the assumption that  $v_\phi$  is independent of  $\theta$ .

In the height-integrated problem considered in the main text, there is a unique frequency associated with convective motions, namely  $N_{eff} = (N^2 + \kappa^2)^{1/2}$ . In the more general problem considered here, there is a multitude of frequencies; indeed, the frequency is a function of two angles, the polar angle  $\theta$  corresponding to the location of a blob, and the angle  $\chi$  associated with the direction of displacement of the blob. (The analysis in the main paper corresponds to the specific choice  $\theta = \pi/2$ ,  $\chi = 0$ .)

In the two-dimensional space of  $\theta$  and  $\chi$ , the value of  $-N_{eff}^2$  varies as a function of the two angles. If  $-N_{eff}^2 \leq 0$  (i.e.  $N_{eff}^2 \geq 0$ ) for all choices of the angles, then the medium is convectively stable. In this case, the convective diffusion constant  $K_c$  is zero and so is the dimensionless constant  $\alpha_c$ . We are not interested in such flows. Rather, we are interested in those flows in which  $-N_{eff}^2 > 0$  for at least some choices of  $\theta$  and  $\chi$ . If we determine the largest positive value of  $-N_{eff}^2$  in such a flow, then  $(-N_{eff}^2)^{1/2}$  would give the growthrate of the most unstable convective mode. We assume that this most unstable mode dominates the convection.

To determine the largest positive value of  $-N_{eff}^2$ , we first differentiate (A2) with respect to  $\chi$  and set the result to zero. We find that the most unstable mode at a given  $\theta$  corresponds to displacements that satisfy

$$\cos 2\chi = \frac{A - B}{[(A - B)^2 + C^2]^{1/2}}, \quad \sin 2\chi = \frac{C}{[(A - B)^2 + C^2]^{1/2}}. \quad (A6)$$

Substituting this value of  $\chi$  back in (A2) we obtain the maximum value of  $(-N_{eff}^2)$  at each  $\theta$ :

$$\left(-\frac{\gamma N_{eff}^2}{\Omega_K^2}\right)_{\theta, max} = \frac{1}{2} \left( (A + B) + [(A - B)^2 + C^2]^{1/2} \right). \quad (A7)$$

Maximizing this quantity next with respect to  $\theta$ , we obtain the overall maximum value of  $(-N_{eff}^2)$ . We find that for all flows that are convectively unstable, i.e. which have  $-N_{eff}^2 > 0$  over at least some range of  $\theta$  and  $\chi$ , the maximum positive value of  $-N_{eff}^2$  occurs at  $\theta = 0$ . Now, as  $\theta \rightarrow 0$ ,  $A$  remains finite, but  $B$  and  $C$  both diverge, with  $B$  diverging faster than  $C$  ( $\cot^2 \theta$  versus  $\cot \theta$ ). This simplifies matters, and so we find that

$$\left(-\frac{\gamma N_{eff}^2}{\Omega_K^2}\right)_{max} = \left(A - \frac{C^2}{4B}\right)_{\theta \rightarrow 0}. \quad (A8)$$

Both in (A7) and (A8), the corresponding mode is convectively unstable only if the quantity on the right hand side is positive. We focus only on such cases.

As noted by QG, the simple “equatorial” analysis presented in the main text of this paper corresponds to using just  $A$  in equation (A8). The more complete analysis presented here shows that the correct expression corresponds to the quantity  $(A - C^2/4B)$ . This is larger than  $A$  because  $B$  is negative. Thus, for instance, it is possible for  $A$  to be negative — which means that the medium is stable to equatorial displacements — and yet displacements at non-equatorial values of  $\theta$  could be unstable, so that the medium as a whole could be convectively unstable. To evaluate (A8), we note that although  $B$  and  $C$  diverge as  $\theta \rightarrow 0$ , the ratio  $C^2/B$  does not, and so  $(-N_{eff}^2)_{max}$  remains finite as  $\theta \rightarrow 0$ . The full expression is

$$\begin{aligned} \left(-\frac{\gamma N_{eff}^2}{\Omega_K^2}\right)_{max} &= 1 - a(\gamma - 1) + [a(\gamma - 1) - (\gamma + 1)]\Omega_0^2 \\ &+ \frac{[a(\gamma - 1) - (\gamma + 1)]^2 \Omega_0^2 (1 - \Omega_0^2)}{2\gamma(1 - \Omega_0^2) + (a + 1)(\gamma - 1)\Omega_0^2}. \end{aligned} \quad (A9)$$

Having determined  $(-N_{eff}^2)_{max}$ , the rest of the analysis proceeds exactly as in the main paper, except that we replace equation (4) for the convective diffusion constant by

$$K_c = \frac{L_M^2}{4} (-N_{eff}^2)_{max}^{1/2}. \quad (A10)$$

Note that this result is valid only if  $(-N_{eff}^2)_{max} > 0$ ; otherwise,  $K_c = 0$ . Just as equation (4) is replaced by (A10), equation (5) is also correspondingly modified. None of the other equations needs to be modified. The radial momentum equation, for instance, is still given by equation (1). For NY-like self-similar flows with  $a = 3/2$  we make use of equation (10), while for the convective envelope solution with  $a = 1/2$  we use equation (12).

The dashed lines in Figs. 1 and 2 show some numerical results. We see that the results are qualitatively similar to what we obtained with the simpler theory presented in the main text (shown by solid lines in the plots). The value of  $\alpha_c$  is larger now compared to the height-integrated theory, as one might expect. The critical  $\alpha_{crit2}$  up to which the convective envelope solution is possible is also larger by a few tens of per cent. Interestingly, the other critical  $\alpha_{crit1}$  is unaffected. When  $\alpha = \alpha_{crit1}$ , the solution has no rotation and the flow is perfectly spherical. In this limit, equatorial displacements capture the full story and the more detailed analysis presented here adds nothing.

The problem considered by QG corresponds to a convectively marginally stable accretion flow in which  $\alpha \rightarrow 0$ ,  $\alpha_c \rightarrow 0$ . They show that in this limit the Bernoulli parameter,

$$Be = \frac{1}{2}v_\phi^2 + \frac{1}{2}v^2 + \frac{\gamma}{\gamma - 1}c_s^2 - v_K^2, \quad (A11)$$

is zero. We confirm this result. The reader is referred to NY, Narayan & Yi (1995a) and Blandford & Begelman (1999) for a discussion of the significance of the Bernoulli parameter. For non-vanishing  $\alpha$  and  $\alpha_c$ , we find that the Bernoulli parameter is always positive. For  $\alpha = \alpha_{crit2}$ , for instance, we obtain  $Be \sim 0.3v_K^2$ .

The positivity of the Bernoulli parameter for finite  $\alpha_c$  in the convective envelope solution is fairly easy to understand once we realize certain properties of these flows. First, in these flows  $v = 0$ , and  $v_\phi$  and  $c_s$  are independent of  $\theta$  (according to the analysis presented by QG which we have borrowed). Therefore, even though the flow rotates and is non-spherical,  $Be$  is nevertheless independent of  $\theta$  and is a function only of  $r$ . Second, the flows we are interested in are convectively unstable. In order to have a convective instability, the Bernoulli parameter has to be a decreasing function of increasing radius. Finally, the flows are self-similar, which implies that  $Be$  must be proportional to  $v_K^2(r)$ . The latter two conditions can both be satisfied only if  $Be$  is positive. Therefore, for finite  $\alpha_c$ , we expect a positive value of  $Be$ . In the limit  $\alpha_c \rightarrow 0$  considered by QG, the flow is marginally stable to convection. This means that  $Be$  must be independent of  $r$ , which can be reconciled with self-similarity only if  $Be = 0$  (as QG found).

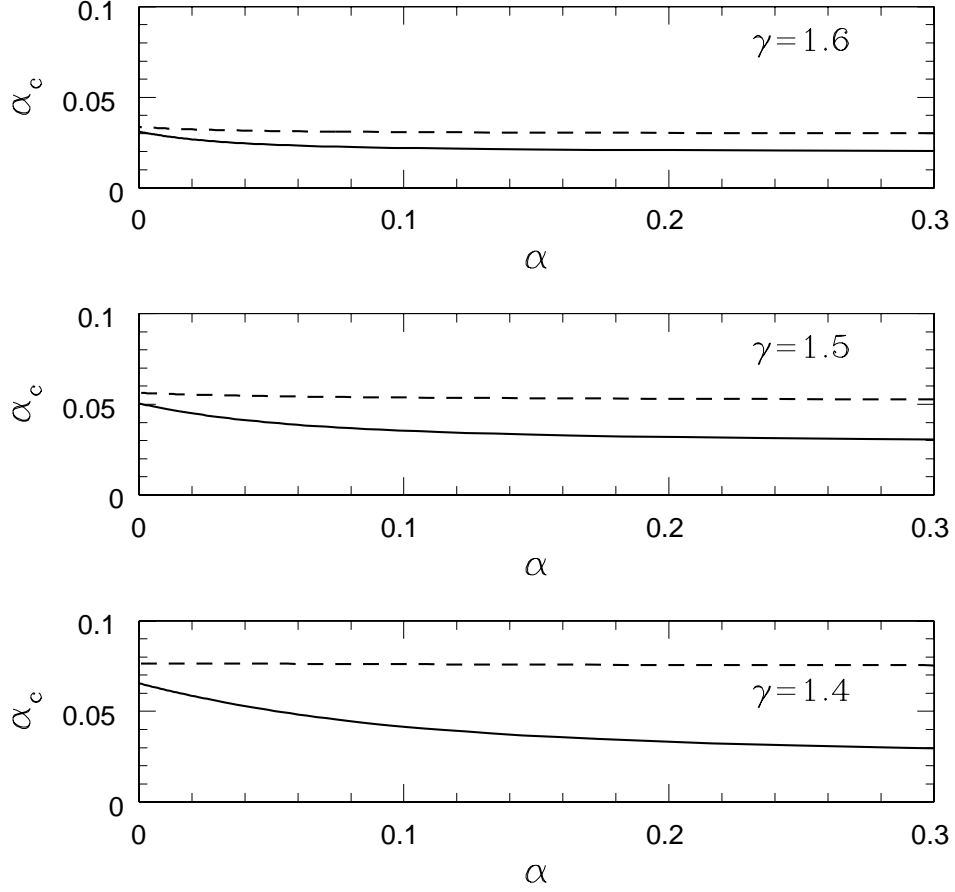


Fig. 1.— Variation of the convective coefficient  $\alpha_c$  as a function of the viscosity coefficient  $\alpha$  for three values of the adiabatic index  $\gamma$ . The calculations correspond to the case when convection moves angular momentum outward according to equation (6). The solutions are of the self-similar form derived by NY, in which the density scales as  $\rho \propto R^{-3/2}$ . Note that there is a consistent solution for all values of  $\alpha$ . The solid lines correspond to the height-integrated version of the theory described in the main paper, and the dashed lines correspond to the analysis described in the Appendix.

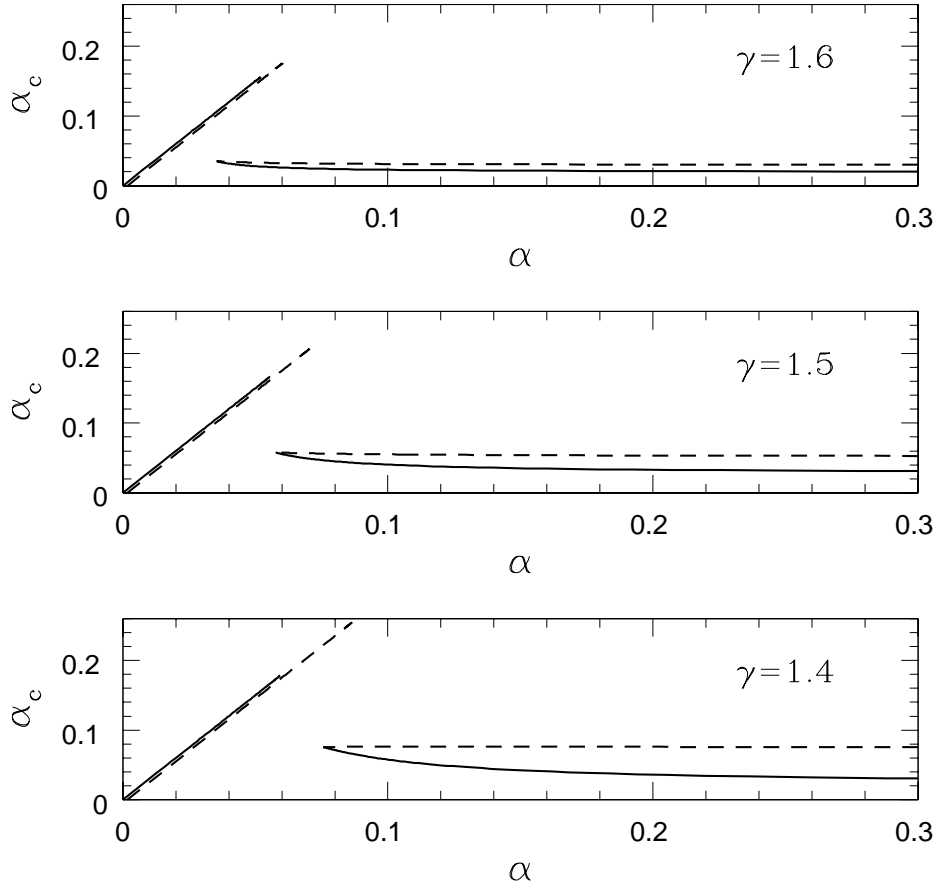


Fig. 2.— Variation of the convective coefficient  $\alpha_c$  as a function of the viscosity coefficient  $\alpha$  for three values of the adiabatic index  $\gamma$ . The calculations correspond to the case when convection moves angular momentum inward according to equation (7). The lines on the right refer to a solution of the self-similar form derived by NY, in which the density scales as  $\rho \propto R^{-3/2}$ . This solution is only available for  $\alpha$  greater than a critical value  $\alpha_{crit1}$ , which depends on  $\gamma$ . The lines on the left correspond to the convective envelope solution discussed in §5.2 in which  $\rho \propto R^{-1/2}$ . This solution is only available for  $\alpha$  less than a critical value  $\alpha_{crit2}$ , which again depends on  $\gamma$ . The solid lines correspond to the height-integrated version of the theory described in the main paper, and the dashed lines correspond to the analysis described in the Appendix.

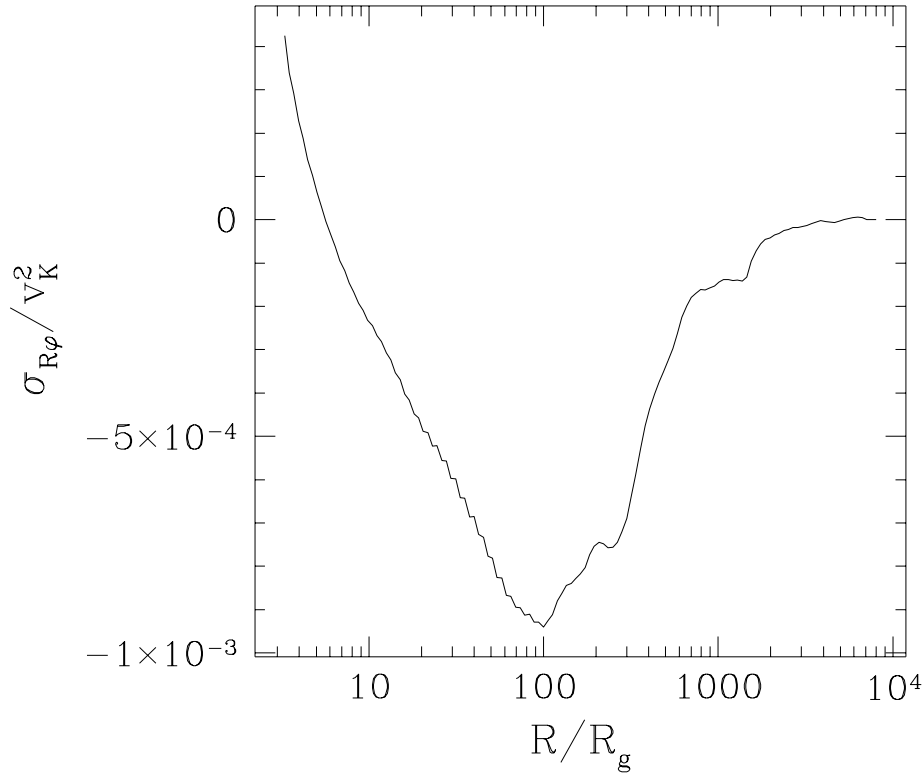


Fig. 3.— Shows the  $(R, \phi)$ -component of the Reynolds stress tensor,  $\sigma_{R\phi}$ , as a function of radius in an axisymmetric numerical simulation of an ADAF with  $\alpha = 0.01$  and  $\gamma = 5/3$ . The Reynolds stress has been averaged over the polar angle  $\theta$  (as explained in the text), and normalized to  $v_K^2$ . Apart from two regions near the boundaries,  $R < 5R_g$  and  $R > 5 \times 10^3 R_g$ , the stress is negative. This confirms that convection in axisymmetric simulations moves angular momentum inward, as argued by Stone & Balbus (1996).

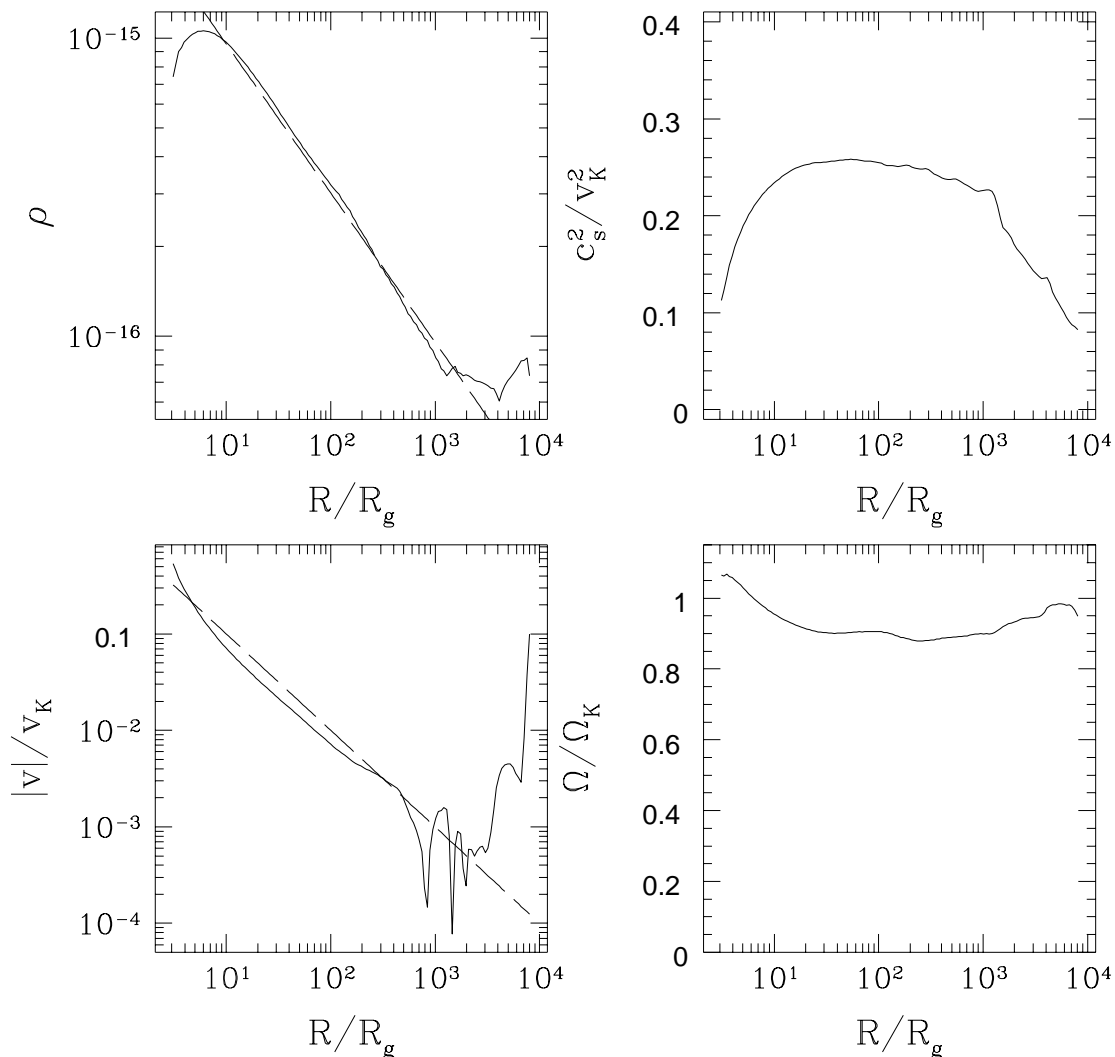


Fig. 4.— Profiles of  $\rho$  (solid line, upper left panel),  $c_s^2/v_K^2$  (upper right),  $|v|/v_K$  (solid line, lower left) and  $\Omega/\Omega_K$  (lower right), shown as functions of radius, for an axisymmetric convectively unstable accretion simulation with  $\alpha = 0.01$  and  $\gamma = 5/3$ . All quantities have been averaged over polar angle  $\theta$  and time. Except near the boundaries ( $R < 10R_g$  and  $R > 10^3R_g$ ), the profiles of  $\rho$ ,  $c_s^2/v_K^2$  and  $\Omega/\Omega_K$  show the power-law behaviors predicted by the self-similar convective envelope solution; also the radial velocity  $v$  is small as predicted. In the upper left panel the dashed line corresponds to the analytical scaling  $\rho \propto R^{-1/2}$ . Similarly, in the lower left panel the dashed line corresponds to the predicted scaling  $|v|/v_K \propto R^{-1}$ .